FEM Simulation of Different Engine Mount Models in an Aircraft Piston Diesel Engine

Paweł Magryta[1*], Konrad Pietrykowski[1], Piotr Borowiec[2]

[1] Department of Thermodynamics, Fluid Mechanics and Aviation Propulsion Systems
Lublin University of Technology, ul. Nadbystrzycka 36, 20-618 Lublin, Poland

[2] Wytwórnia Sprzętu Komunikacyjnego „PZL-Kalisz" S.A., ul. Częstochowska 140, 62-800 Kalisz, Poland

* Corresponding author's e-mail: p.magryta@pollub.pl

ABSTRACT

The article presents the results of numerical simulations using the FEM (Finite Element Method) of the engine mount strength for mounting an aircraft diesel engine with opposite pistons called PZL-100. Four versions of the mount prepared by aircraft engine producer WSK "PZL-Kalisz" company were analyzed. Tests were performed in Catia v5 software in the Generative Structure Analysis module. The boundary conditions were engine gravity force, propeller thrust force, and propeller torque. S235JR steel was defined as the material. A design grid with tetrahedral elements with a single element size of 2 mm was used. As part of the simulation study, four structural solutions for the test engine mounts were calculated in terms of strength. The results of stress maps and the magnitude of deformation of the mount elements were compared. Based on the obtained results, one of the mount versions was recommended for actual fabrication.

Keywords: engine mount, diesel engine, aircraft, FEM

INTRODUCTION

This paper presents the results of mathematical calculations of the strength of several versions of the PZL-100 aircraft diesel engine mount developed at WSK "PZL-Kalisz" company. The PZL-100 three-cylinder two-stroke compression-ignition engine has 3 cylinders, 6 pistons, and 2 crankshafts. It is an opposite piston engine with uniflow scavenging. The maximum continuous power of the engine is 100 kW, with the rotational speed of the crankshafts of 4000 rpm reduced to 2400 rpm on the propeller shaft. This work is a continuation of the work presented in the article [1]. The presented mount will be used for static tests of the engine and will not be used for flight.

In the scientific literature, there is a lack of works describing the strength testing of mounts used in the aviation industry. This is mainly because engine mounts are custom-made for aerospace parts manufacturers. These companies do not analyze mounts for strength using simulation tools. The exception are mounts developed as part of research work involving scientific units. This kind of approach is presented in this article. It should be noted that the work is carried out in conjunction between the contractor (industry) and the research unit (university), which further contributes to the expansion of cooperation.

The process of designing the engine mount is often supported by mathematical modeling. It is used at every stage of engine design. In the conceptual phase, one-dimensional models such as AVL Boost [2, 3, 4] are used, followed by three-dimensional flow modeling using CFD (Computational Fluid Dynamics) [5] and modeling the strength of the structure using the FEM (Finite Elements Method) [6, 7, 8]. The article [9] describes the small engine block design method used in the Zlin 26 sports plane. The calculations were made in the PTC ProE Mechanica software. However, the report [10] presents the FEM

analysis of the engine mount performed in the Cosmos-M software.

The tests aimed to check the strength of the structure for all engine operating conditions. In many cases, the mount is developed technologically simultaneously with other aircraft components, such as the main gearbox. This approach is presented in the publication [11], where the authors performed strength simulations of these two components simultaneously in simulation software. A key aspect also seems to be a more thorough analysis of welded joints, which are the most vulnerable in a mount structure, as the publication's authors [12]. Model tests help to choose the best version or indicate the necessary structural corrections, even before the actual mount is made. This is important because a mount failure during testing can lead to engine failure and a consequent increase in engine development costs and time. Similar studies to those presented above have been performed not only for engine mounts but also for other load-bearing structures [13]. Another interesting approach is the possibility of analyzing the entire prototype structure for strength analysis, as presented for composite material and a floating ship mount in the publication [14]. Suppose a given mount component lacks adequate strength. In that case, it can fail, as shown in the publication [15], where the authors analyzed the material of the engine mount bracket and then modified its design and, using FEM simulation tools, checked its strength. There are also publications describing strength analyses of mounts for the automotive industry. Such work is presented in the publication [16], which includes a comprehensive strength analysis of an engine mount used in an automobile.

Internal combustion engines are tested on an engine dynamometer. During the test, the engine's power must be received by some receiver to measure the engine performance over its entire operating range. Usually, special engine brakes are used for this purpose. This kind of solution has been presented in publication [17], in which the authors have tested a prototype of an aircraft opposed-piston engine with various values of intake pressure. Another example can be a publication [18] where the authors checked the effect of pre-chamber volume on the combustion characteristics of an SI aircraft piston engine. When testing aircraft engines, instead of the brake, a propeller with adjustable pitch is often used by adjusting the angle of the blades. This allows to examine the so-called propeller characteristics, i.e., made with a constant propeller pitch. Thanks to this, the test conditions are similar to those during the flight. Using a propeller as a load on the engine also allows for examining the drive system.

The torque transmitted to the propeller cannot be measured directly. The equivalent reaction torque acting on the engine block and the supports are measured to calculate the torque produced by the engine. Unique stands are used on the test bench of aircraft engines, allowing for pivoting engine mounting and measuring the reaction torque.

The aircraft engine is attached to the post via a mount. The mount structure used during the bench tests is similar to that used in airplanes. However, the mount does not have to meet the weight requirements, so it can be made of cheaper and more available materials. During the tests, the mechanical loads generated by the engine may be greater than those in flight. On stands, engines are tested in a wide range of loads that are not used during flight. The engine mount should be able to withstand these loads without the risk of damage. At the same time, it should remain stiff.

MODEL DESCRIPTION

This paper presents the results of a simulation study of the strength of a mount for mounting a research engine. The research object is more extensively described in publication [19]. Compared to the article [1], this paper describes four successive versions of the mount for mounting the research engine, which was prepared by the manufacturer of the PZL-100 engine, the company WSK "PZL-Kalisz". The models consist of tubing, engine mounts, and a test bench connected by welded joints. It was assume that the engine mount will be welded using fillet welds. The welds were mapped in geometric models. Figure 1 shows the CAD model of the engine with the engine mount 3. All the mount geometries and their modifications are shown in Figures 2 and 3. The mount modifications consisted mainly in changing how the mount is restrained to the rear flat wall to which it will be mounted during bench tests. However, the spacing of mounting holes and their placement were also changed. Changes in the attachment of the side tubes in each mount were also apparent.

The arrangement and size of the engine's components to the mount remained the same.

Wide and flat mounts characterized the version of mount 1 to the rear wall. A flat piece is also visible at the top of this mount for mounting the test engine controller. It was removed in subsequent versions due to a change in the mounting of this electronic unit. Mount 1 also has additional reinforcements in the upper lateral part in the form of intermediate tubes connecting the upper and lateral parts of the truss.

Mount 2 is a mount with a smaller distance between the attachment points to the back wall than version 1. The size of the attachments to the back wall is the smallest in this version.

Mount 3 is a mount with the smallest distance between the attachment points to the rear wall. It is characterized by the enlarged shape of the attachment to the back wall, which changes the angles of the side tubes.

Mount 4 has the direction of the sidpipes reversed but is characterized by an increased distance between attachment points compared to mount 3.

As in the performance of previous calculations, the same boundary conditions, shown in Figure 4, were adopted in this study for the different versions of the framework and subsequent calculation steps. This situation allows direct comparison of the following simulation results with each other. All calculations were performed in Catia v5 software in the Generative Structure Analysis module. The same immobilization and loading conditions, as well as the same material properties, were given for each version of the mount:

- Gravity force equal to 1000 N corresponding to the engine mass of 100 kg estimated from the developed geometric models was assumed.
- Propeller thrust force 5000 N, a value corresponding to the value of propeller thrust at maximum engine power, was assumed.
- Torsional torque of the engine 227 Nm, a value corresponding to the reaction torque from the propeller torque, was assumed.

Table 1 presents the primary material data for the material adopted, which is S235JR steel. Such steel was proposed by the entrepreneur WSK PZL Kalisz due to its availability. The use of a better material would favorably increase the safety factor, but this was not considered at this stage of the work.

A Mesh grid with a single Tetrahedral type element size of 2 mm was adopted for the calculations. This type of element was chosen because of the complex geometry at the pipe connection point. The reasonableness of its size was the subject of simulation studies at an earlier stage of the work. It was shown that for this geometry size, it is reasonable to use a mesh with an element size of 2 mm. Successive reduction of the element size did not affect the obtained results but only increased the simulation time. An example view of the finished calculation mesh for mount 2 is shown in Figure 5.
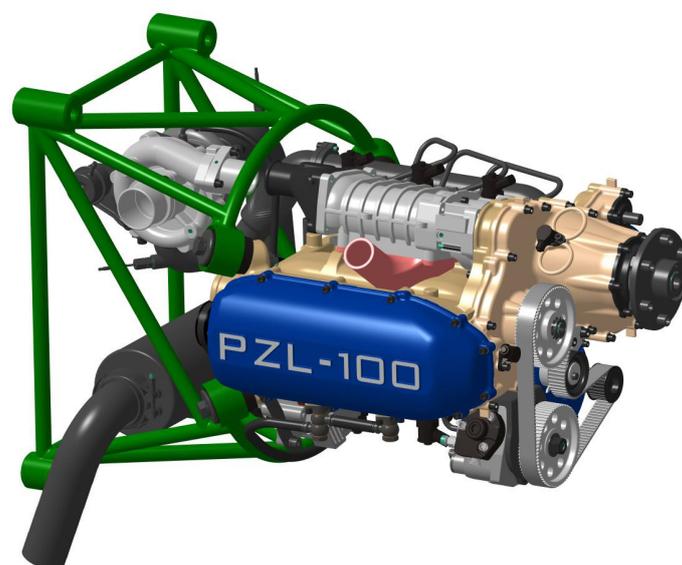

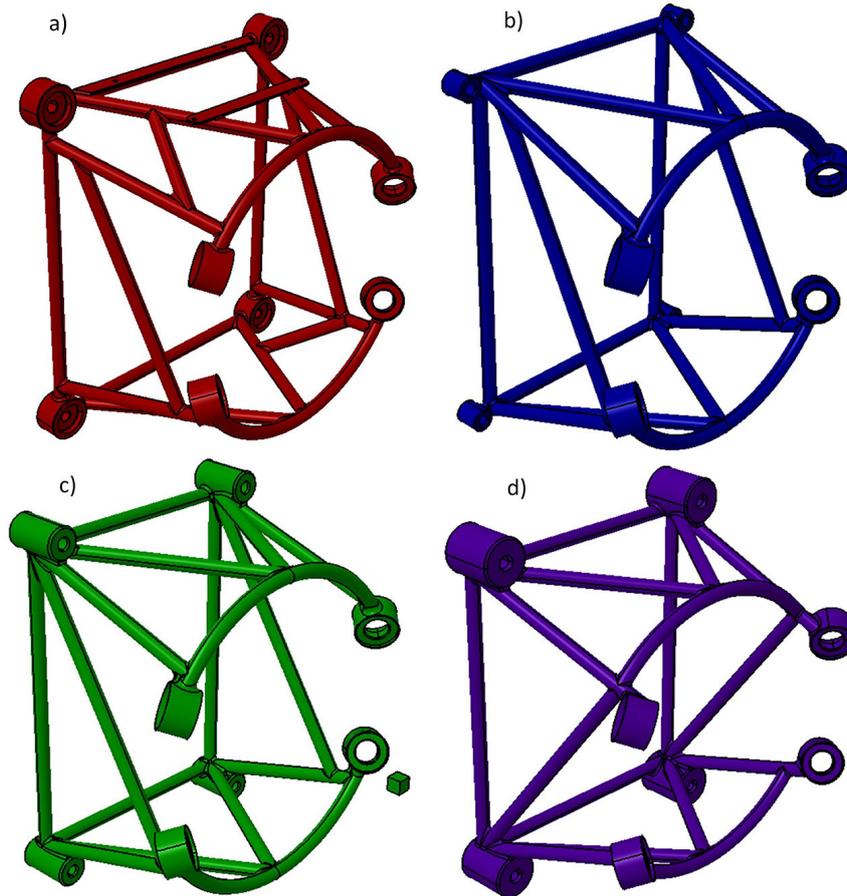**Fig. 1**. CAD model of the PZL-100 engine with the engine mount 3

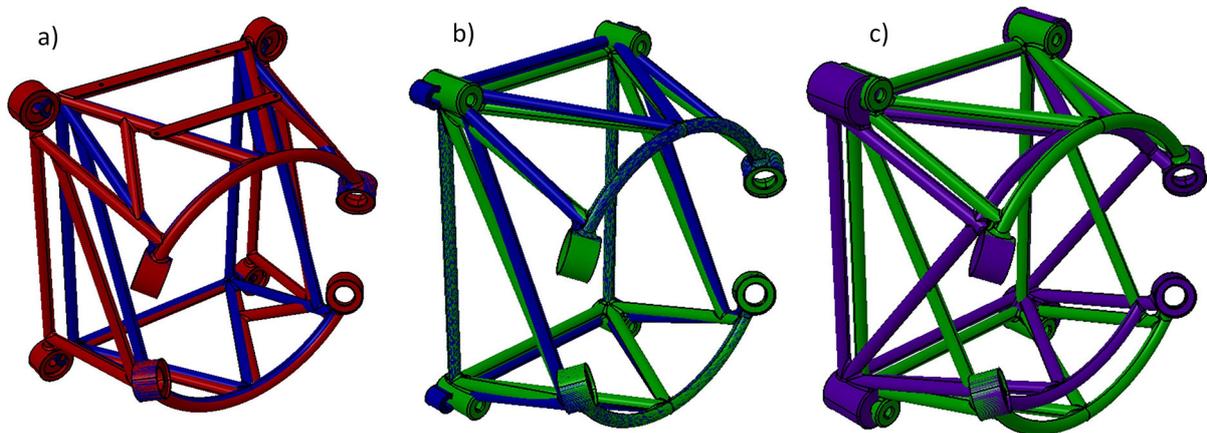**Fig. 2**. Successive mount versions – a) mount 1, b) mount 2, c) mount 3, d) mount 4

Fig. 3. Subsequent mount versions – comparison in the chronological cycle –
a) mount 1 – mount 2, b) mount 2 – mount 3, c) mount 3 – mount 4

RESULTS

The results are divided into four subsections, each of which presents the results of simulation studies in the form of stress distributions of mounts 1, 2, 3, and 4.

Mount 1

Figure 6 shows the results of stress distributions for mount 1. For better visibility of the results, the scale was limited to 25 MPa. The results show that the stresses on most structures are
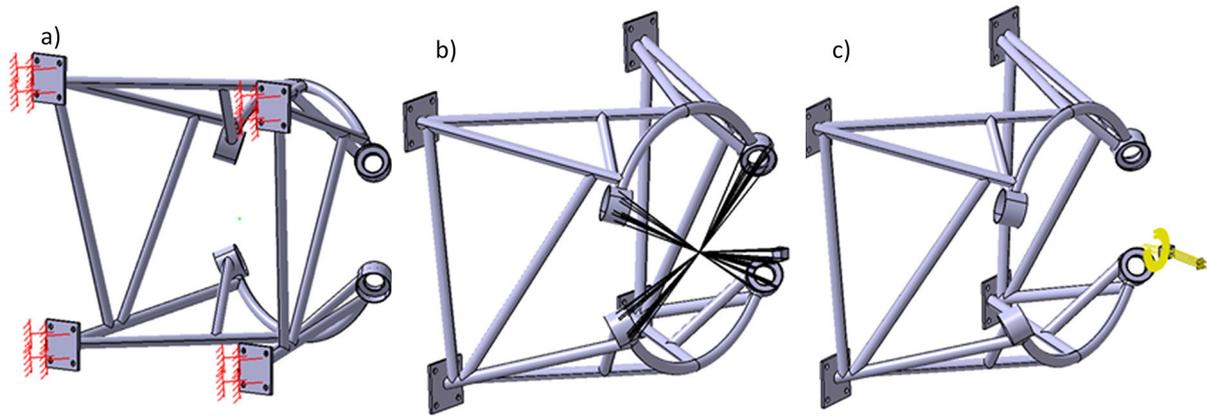
Fig. 4. Restraint and load boundary conditions – a) restraint, b) stiffness bond, c) load [1]

Table 1. Material data of S235JR steel [20]

Young's modulus	210 GPa
Poisson number	0.3
Density	7800 kg/m³
Minimum yield strength of ReH	235 MPa
Strength limit Rm	360-510 MPa

minimal (blue color). However, there are places where they reach values above 100 MPa. The highest stress values are found at the joints of the mount components (red), especially in the welds between the tubes, the motor mounts, and the test stand mounts. This is due to the notches that form at welded joints, where there is a rapid change in shape. In addition, the stress pile-up is influenced by the fact that the mounting elements have a higher stiffness than the connecting elements (tubes). Significant stresses also occur along the length of the top and bottom tubes (green color, about 10 MPa). In the case of the top tubes, this is due to tensile force, and in the case of the bottom tubes, to compressive strength.

Figure 7 shows the location of the maximum stress value for mount 1. The maximum stress values, in reality, would not reach those obtained in FEM studies. They result from simplifications, such as the presence of sharp edges at the joints of elements and the restriction of the minimum size of the elements of the calculation grid to 2 mm.

Mount 2

Figure 8 shows the results in the form of stress distributions for mount 2. This mount differs from mount 1 mainly in using smaller, and therefore less rigid, mounting elements for the test stand and the absence of transverse tubes to stiffen the entire structure. This had a favorable effect on stress distribution. In this version, the main connection elements are loaded evenly along their length (green, about 10 MPa). It is also noted that mainly four tubes carry the load. In addition, the stresses on the left lower tube are the smallest of the four. This is due to the action of the reaction torque of the engine, acting in the right direction.
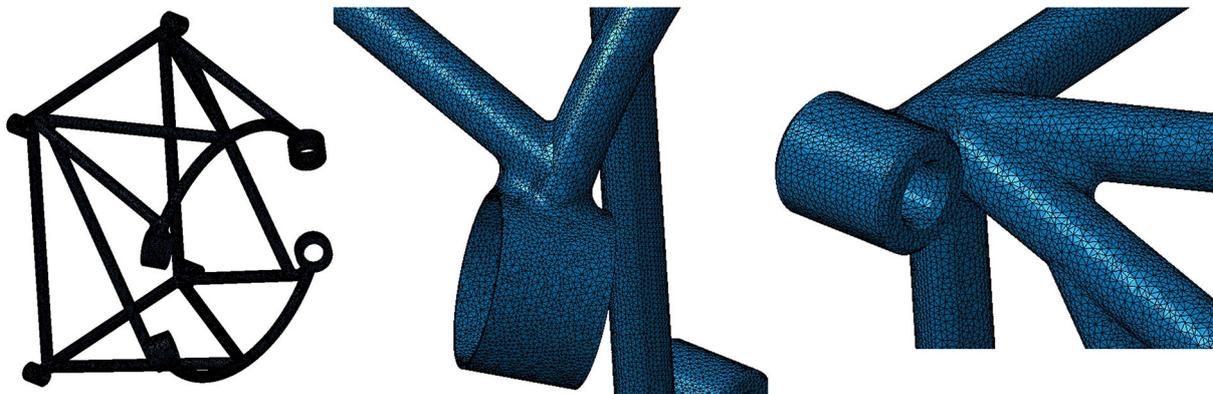

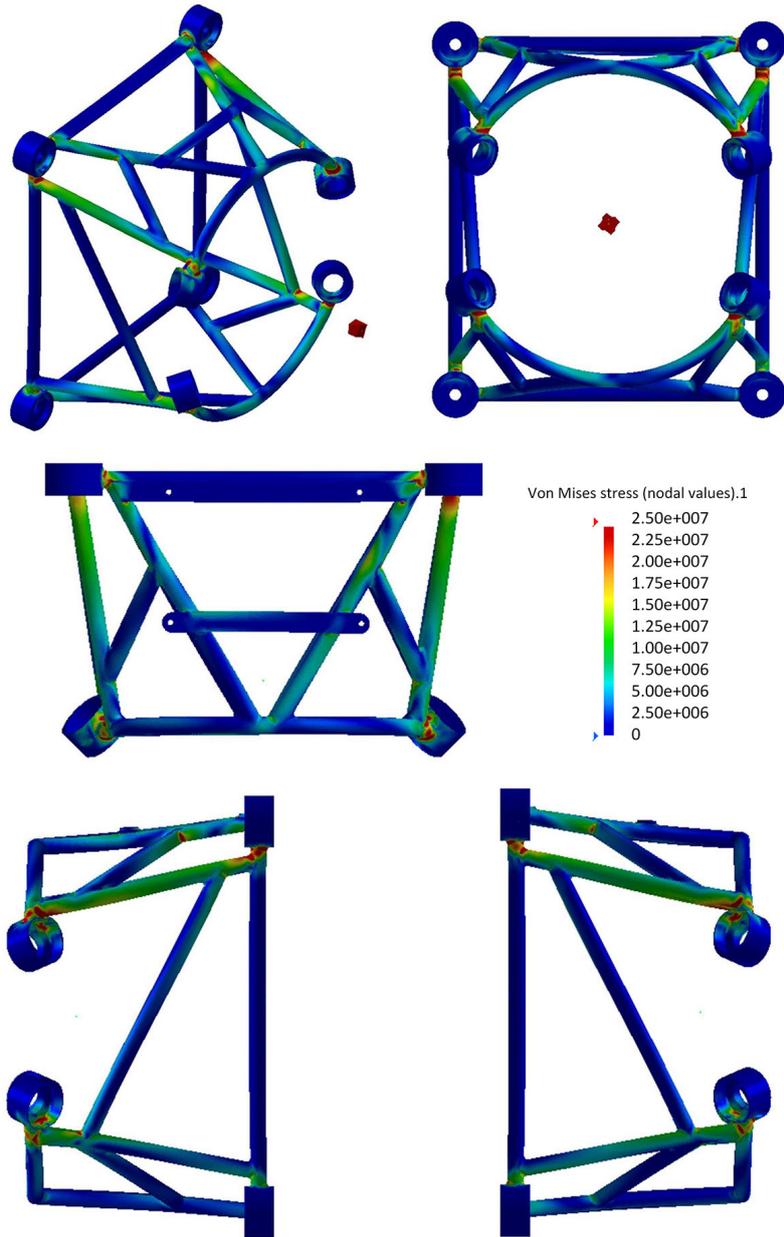**Fig. 5**. Mesh grid on the example of mount 2

Von Mises stress (nodal values).1

| 2.50e+007 |
| 2.25e+007 |
| 2.00e+007 |
| 1.75e+007 |
| 1.50e+007 |
| 1.25e+007 |
| 1.00e+007 |
| 7.50e+006 |
| 5.00e+006 |
| 2.50e+006 |
| 0 |

Fig. 6. Results in the form of stress maps for mount 1

Von Mises stress (nodal values).1 Global Maximum.1 1.05978e+008 N/m^2

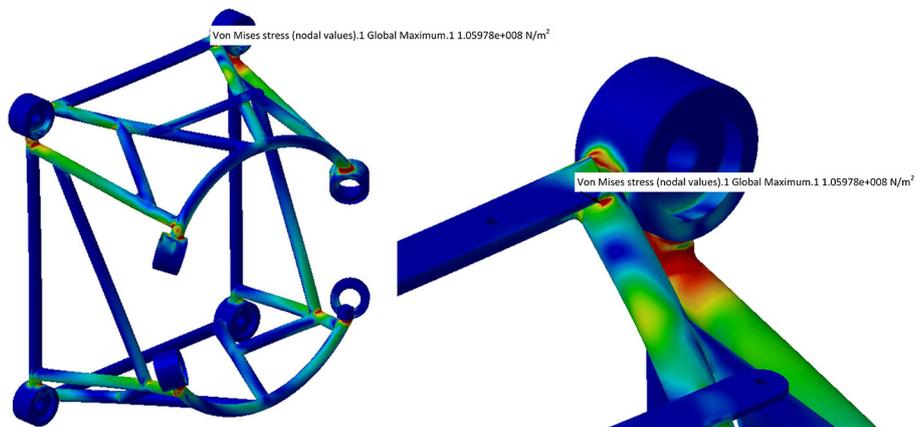Von Mises stress (nodal values).1 Global Maximum.1 1.05978e+008 N/m^2

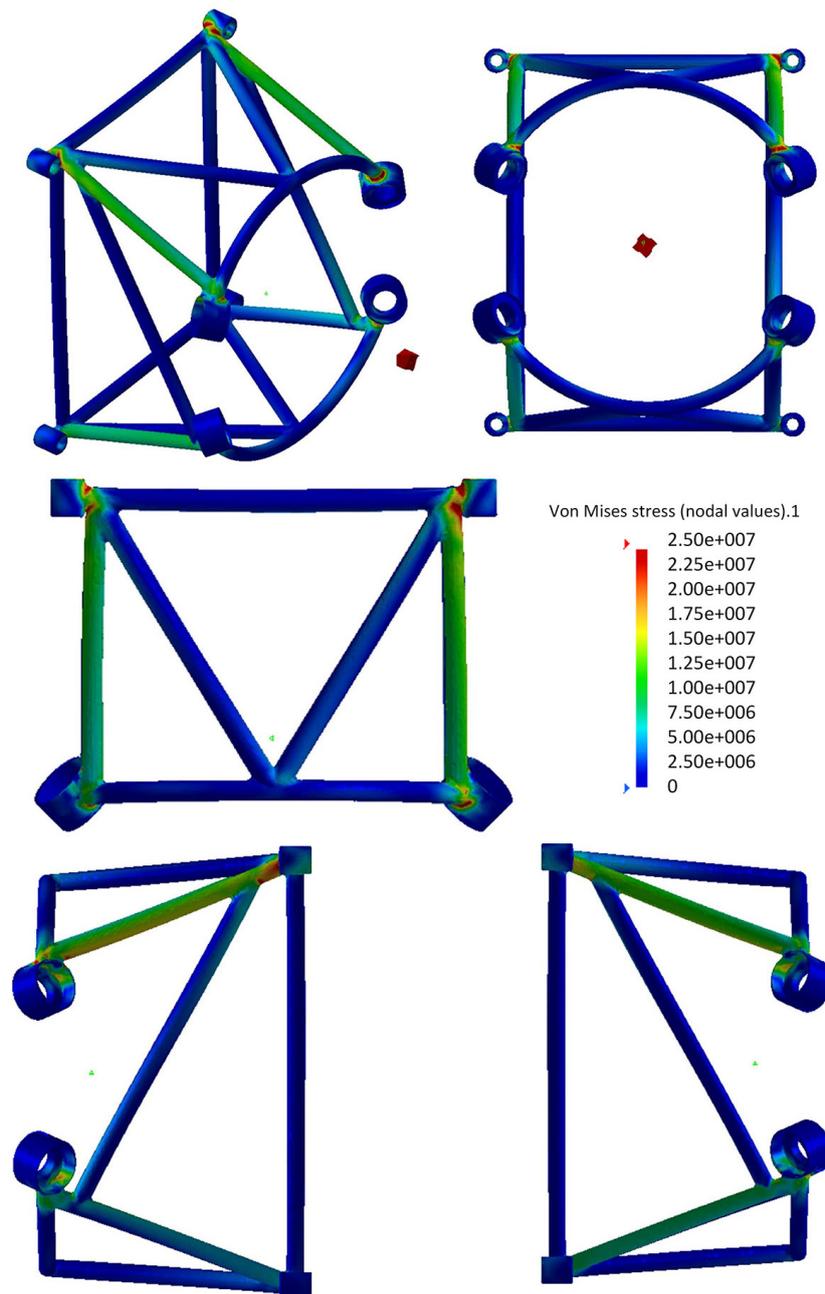**Fig. 7**. Closer results in the form of stress maps for mount 1

Fig. 8. Results in the form of stress maps for mount 2

Figure 9 shows the location of the maximum stress value for mount 2. The maximum stress values have decreased compared to the previous mount version to about 64 MPa. This is due to a reduction in the stiffness of the mounting elements to the test stand.

Mount 3

Figure 10 shows the results of stress distributions for mount 3. The mounting elements to the test stand were lengthened in the next mount version to transfer the tube connections precisely to these elements. This reduced the stresses on the tubes between the mounting elements to the stand. This decreased the maximum stresses to about 48 MPa. They are located in this mount version near the connections on the engine mounting elements.

Figure 11 shows the location of the maximum stress for mount 3. It is noted that the maximum stresses are distributed over a certain length around the connections on the engine mounting elements, which is beneficial for the strength of the structure.
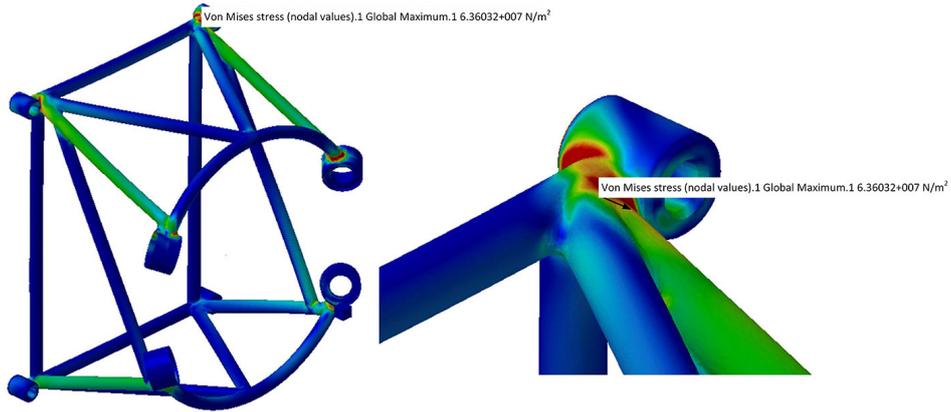
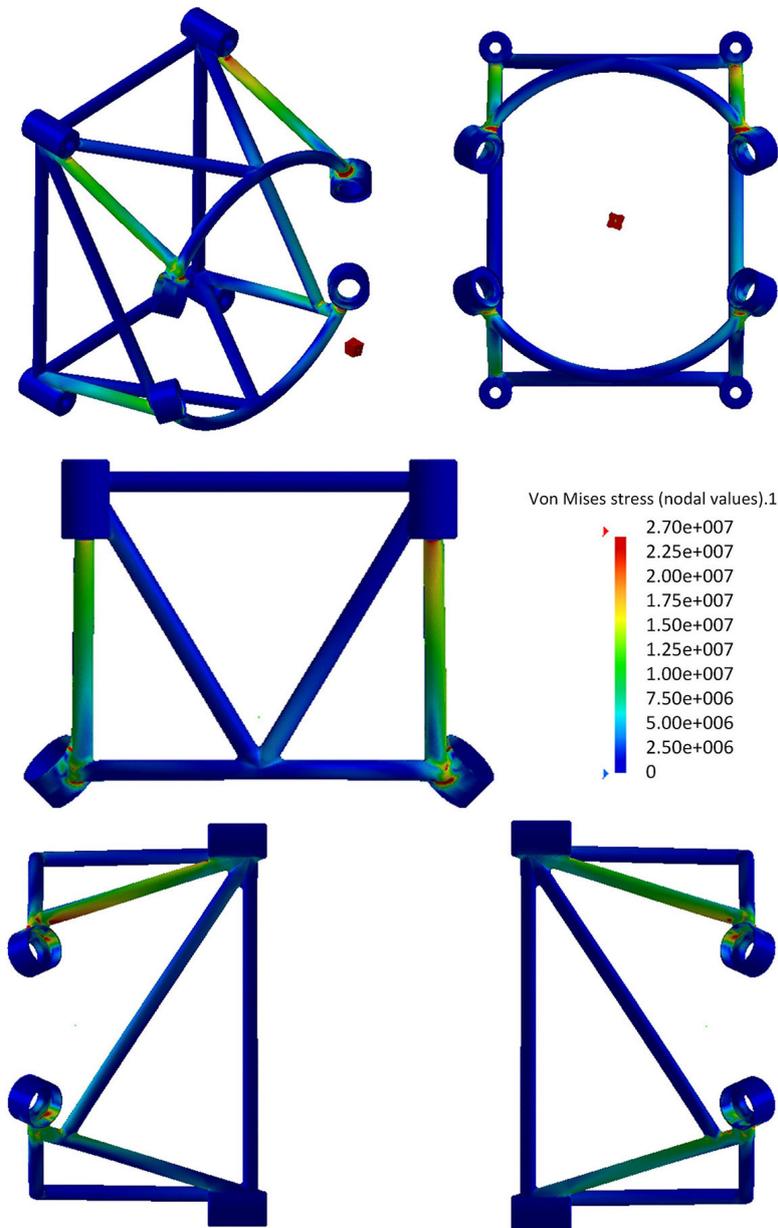**Fig. 9**. Closer results in the form of stress maps for mount 2

Fig. 10. Results in the form of stress maps for mount 3

Von Mises stress (nodal values).1 Global Maximum.1 4.84726e+007 N/m²

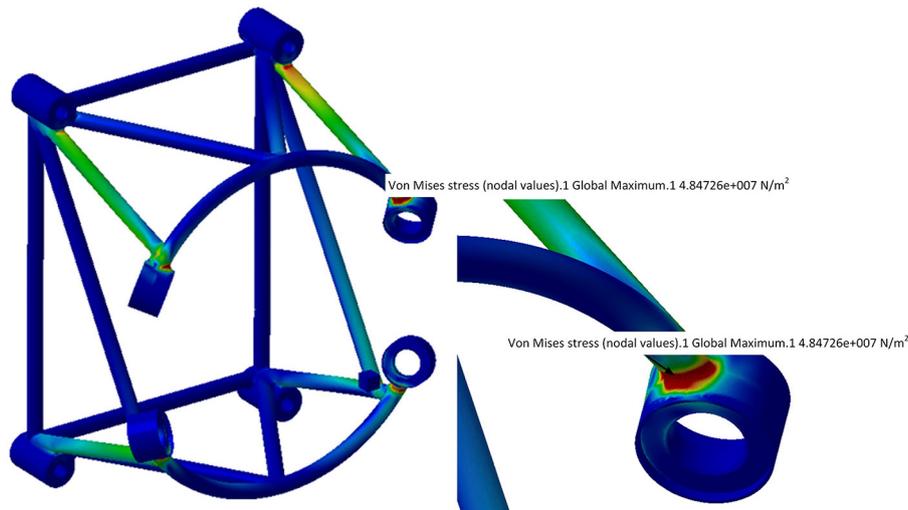Von Mises stress (nodal values).1 Global Maximum.1 4.84726e+007 N/m²

Fig. 11. Closer results in the form of stress maps for mount 3

Mount 4

Figure 12 shows the results in the form of stress distributions for mount 4. This mount version used mounting elements for the stand with a larger diameter. The purpose of this was to increase the external surface area of these elements and, consequently, to facilitate the welding process of the mount. This did not significantly affect the stress distribution. It should be noted that the weight of the entire mount was increased this way; however, the mount is intended for mounting the engine on the test stand, and its weight is not essential.

Another design modification was introduced: moving the bent tubes connecting the motor mounts backward. This caused a local increase in the stresses on the connecting elements. Figure 13 shows the location of the maximum stresses for mount 4. They increased to about 58 MPa compared to the previous mount version.

DISCUSSION

The simulation studies presented above analyzed four structural solutions for the test engine mounting mounts for strength. In all mounts except mount 1, the maximum stresses did not exceed 64 MPa. In mount 1, these stresses amounted to 106 MPa, but this is due to the occurrence of these stresses at the interface between the tube connection and the engine controller mounting element. This is because this element, in the form of a flat bar, is connected to the tubes located on

the sides of the mount and is bent. The motor driver mounting element is not present in mounts 2, 3, and 4.

For a recommendation to be made in the best-suited mount 3. It is characterized by the lowest values of maximum stresses of 48.47 MPa. These occur at the weld at the pipe connection at the motor mounting bracket. This value of maximum stresses is acceptable. It can be compared with the results presented in the publication [21], where the authors reduced the maximum stress in the engine mount to 51.75 MPa and considered the structure safe. Similar to the publication's authors [22], reducing the maximum stress in the drive unit mounting by 35% was possible. Implementing the four versions of the mounts described in this article made it possible to select the version with the smallest values of maximum stresses.

As shown in the publication [23], numerical calculations used to check the strength of fastening elements of drive units are very useful in verifying the design assumptions. In addition, they significantly shorten the process of designing the finished product.

In addition, verification calculations were performed to check the correctness of the calculations performed for this version of the mount. The Mesh calculation grid was compacted to a single element size of 1 mm at the locations of maximum stresses, i.e., at the welds of the connections between the pipes. Such compaction did not significantly increase the maximum stress values.

A similar distribution of stresses characterizes all tested mounts. The most stressed are
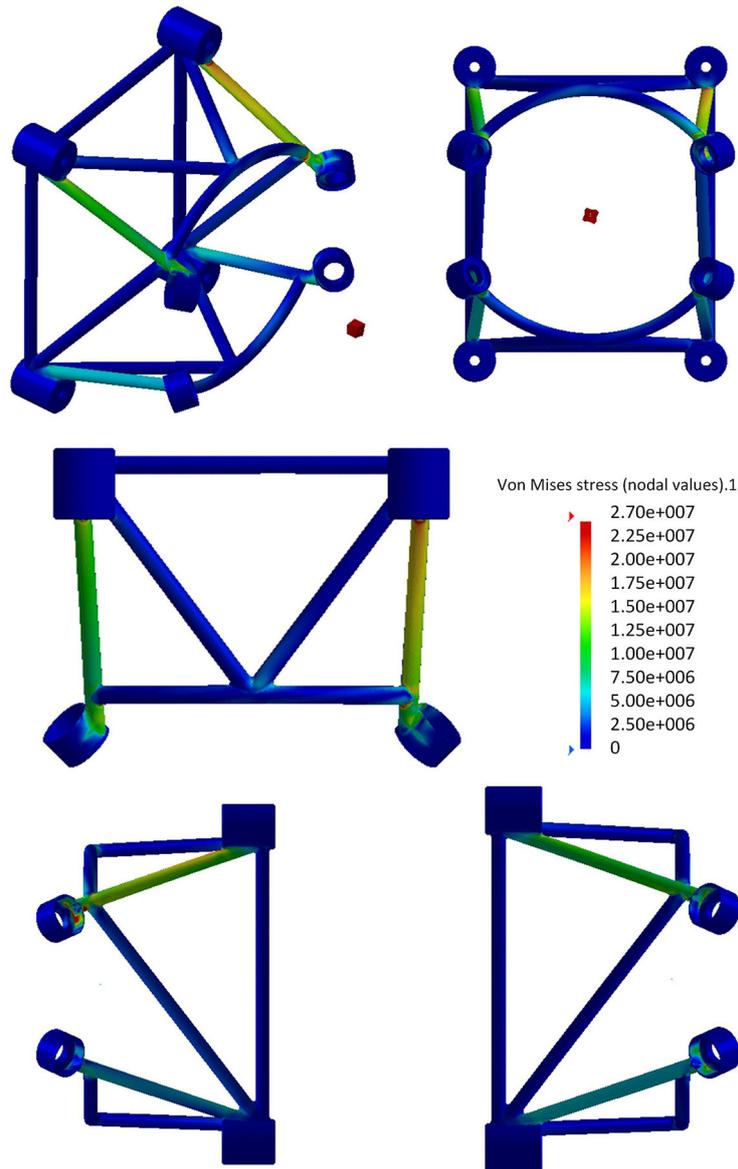
Von Mises stress (nodal values).1

▶	2.70e+007
	2.25e+007
	2.00e+007
	1.75e+007
	1.50e+007
	1.25e+007
	1.00e+007
	7.50e+006
	5.00e+006
	2.50e+006
▶	0

Fig. 12. Results in the form of stress maps for mount 4

Von Mises stress (nodal values).1 Global Maximum.1 5.77836e+007 N/m²

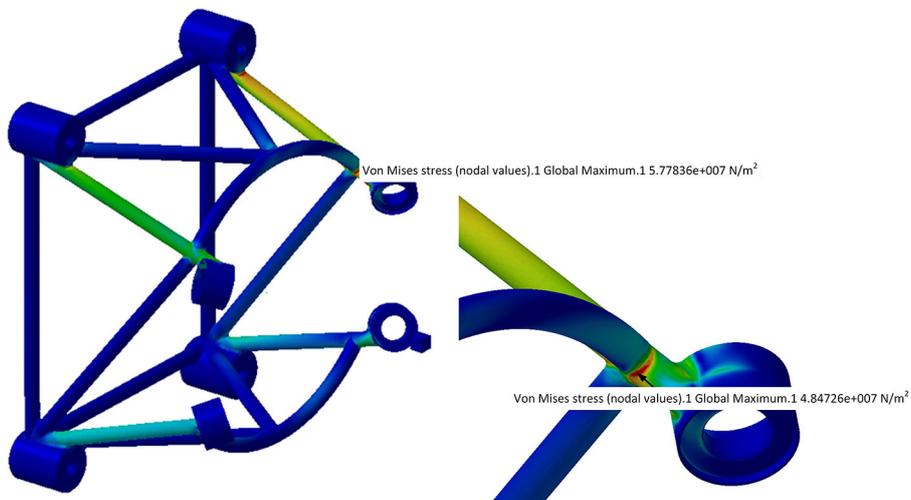Von Mises stress (nodal values).1 Global Maximum.1 4.84726e+007 N/m²

Fig. 13. Closer results in the form of stress maps for mount 4

the tubular elements located s the upper part of the mount, and the highest stresses occur at the connection of the two upper tubes with the elements of attachment to the engine and the fuselage of the air mount, mainly where welds appear. Attention should be paid to correct welding technology and due diligence in manufacturing these elements (PN-EN 1011-2:2004 standard), as well as a correct and detailed inspection process for welded joints (PN-EN ISO 15614-1:2017-08 standard).

An additional possibility may be using a different material or a thinning of the structure, which may be helpful when the presented solution is used in a flying vehicle. This approach was presented in the publication [24], where the material change from steel to aluminium reduced 17.9% of the element's weight. However, in the current solution, the mount will be used for static tests of the engine and will not be used for flight. Therefore the authors did not propose to change the material.

It should also be mentioned that the simulations performed included static loads. Therefore, it is necessary to carry out further research to verify the mount's resistance to dynamic loads.

It should also be emphasized that based on the tests carried out, it is not possible to obtain an exact answer as to whether the strength reserve obtained during the presented static simulation tests will allow safe operation under dynamic engine operating conditions. This issue will be the subject of future research work.

However, the maximum stress in mount No. 3 was about 48 MPa, which, compared with the minimum yield strength of ReH which for the adopted material is 235 MPa, allows us to estimate a safety factor of close to 5. It should be emphasized that in the case of strength calculations, the selection of safety coefficients should be interpreted individually for each element, as demonstrated by the authors in the publication [25], in which the rotor hub of an unmanned helicopter was subjected to performance analysis.

CONCLUSIONS

The analysis shows the following conclusions:
- Numerical calculations allow for a quick comparison of several similar structures in terms of strength and facilitate the selection of the best solution.
- Maximum stresses in the welded engine mount were observed at the welded joints.
- The maximum stress of 106 MPa was obtained for engine mount 1. The maximum stress level for all tested structures is much lower than the minimum yield strength of the material used.
- The safety factor of close to 5 is achieved for engine frame 3 but can be increased by using better material.
- The resulting safety factor is greater than the value of the safety factor for the design operating under dynamic loading conditions, for which it should be in the range of 3.5-4.0 [26].
- Average values were assumed as boundary conditions for the design, due to the lack of knowledge of the amplitude of dynamic loads (the object is a diesel engine lighter), which in real life may be several microns higher.

REFERENCES

1. Magryta P., Pietrykowski K. Simulation research of the strength of an engine mount in an aircraft piston diesel engine. Journal of Physics; Conference Series; 2021; 2130: 012017.

2. Grabowski Ł., Pietrykowski K., Karpiński P. The zero-dimensional model of the scavenging process in the opposed-piston two-stroke aircraft diesel engine. Propulsion and Power Research; 2019; 8 (4).

3. Magryta P., Pietrykowski K., Gęca M. Thermodynamic Model of the ASZ-62IR Radial Aircraft Engine. Transactions on Aerospace Research; 2018; 2018 (1): 36-48.

4. Czyż Z., Grabowski Ł., Pietrykowski K., Czarnigowski J., Porzak M. Measurement of flight parameters in terms of toxic emissions of the aircraft radial engine ASz62-IR. Measurement; 2018; 113: 46-52.

5. Biały M., Pietrykowski K., Tulwin T., Magryta P. CFD numerical simulation of the indirect cooling system of an internal combustion engine. Combustion Engines; 2017; 170(3): 8-18.

6. Pietrykowski K., Magryta P., Skiba K. Finite element analysis of a composite piston for a diesel aircraft engine. Combustion Engines; 2019; 179(4): 107-111.

7. Stoklosa R. Aircraft Engine Mount – Frequency/Vibration Testing. Solid Works Tech blog; 2018.

8. Lisitsin O. Aspects of the Light Aircraft Engine Mounts Strenght analysis. Engre Engineering Elements Blog; 2020.

9. Jurek M., Judičák J. Design and analysis of engine mount for the use of modern-design engine in small sport plane Zlin 26 Series. Acta Avionica; 2013; 15(27).

10. Engine mount analysis report. Report No ER-01002; 2003.

11. Ly D. Nguyen, Taison K., Remo N. A Methodology to Analyse Aircraft Engine Gearbox and Mounting System Simultaneously Using Finite Element Analysis. SAE Transactions; 2002; 111(1): JOURNAL OF AEROSPACE: 601-608.

12. Guillaume M., Schläpfer E., Schmid M. Structural Analysis of Ageing Pilatus P-3 Engine Mount. Procedia Engineering; 2015; 114: 583–589.

13. Lokwic P. Optimisation of the Lift Carrying Frame Construction by Using Finite Element Method. Advances in Science and Technology Research Journal; 2018; 12(4): 207–215.

14. Markuszewski D., Wądołowski M., Gorzym M., Bielak M. Concept of a composite frame of martian vehicle. Advances in Science and Technology Research Journal; 2021; 15(4): 222–230.

15. LongH., Zhang B., Su J., Deng Q. Failure analysis of engine mounting bracket of a passenger car. Engineering Failure Analysis; 2022; 136: 106190.

16. Adkine A. S., Overikar G. P., Surwase S. S. Modal analysis of engine supporting bracket using finite element analysis. International Journal of Advanced Engineering Research and Science (IJAERS); 2017; 4(3): 55-63.

17. Mazuro P., Kozak D. Experimental investigation on the performance of the prototype of aircraft Opposed-Piston engine with various values of intake pressure. Energy Conversion and Management; 2022; 269: 116075.

18. Huasheng C., Zhenfeng Z., Fujun Z., Chuncun Y. Lei W. Effect of pre-chamber volume on combustion characteristics of an SI aircraft piston engine fueled with RP3. Fuel; 2021; 286: 1(15).

19. Biały M., Grabowski Ł., Skórzyński B., Barański G., Majczak A. Analyzing mechanical vibrations of an aircraft opposed piston engine. Combustion Engines; 2021; 187(4): 3–7.

20. https://metinvestholding.com/pl/products/steel-grades/s235jr

21. Lakshmankumar A., Balasivaramareddy K., Sathiskumar A., Kuthus. Stress analysis and optimization of engine mount. International Journal of Mechanical Engineering and Technology (IJMET); 2017; 8(6): 148-155.

22. WU K., LING L., HAN Ch. Design of GFRP Engine Mount Frame by Using Topology Optimization. In: Proc. of 2nd Annual International Conference on Advanced Material Engineering, Wuchan, China, 1243-1250.

23. Alkhatib F. Techniques for engine mount modeling and optimization. University of Wisconsin Milwaukee UWM Digital Commons. 2013.

24. Ramesh S., Handal R., Jensen M. J., Rusovici R. Topology optimization and finite element analysis of a jet dragster engine mount. Cogent Engineering; 2020; 7(1).

25. Cygnarowska K., Czyż Z., Karpiński P., Skiba K. Strength analysis of the rotor hub of an unmanned helicopter. Journal of Physics: Conference Series, 2021, 1736.

26. Ligaj B. Materiały do ćwiczeń z Podstaw Konstrukcji Maszyn.